



UNIVERSITY
OF WOLLONGONG
AUSTRALIA

University of Wollongong
Research Online

Faculty of Engineering - Papers (Archive)

Faculty of Engineering and Information Sciences

2009

Development of a force sensor working with MR elastomers

Weihua Li

University of Wollongong, weihuali@uow.edu.au

Kosta Kostidis

University of Wollongong

Xianzhou Zhang

University of Wollongong, xianzhou@uow.edu.au

Yang Zhou

University of Wollongong, yz248@uow.edu.au

<http://ro.uow.edu.au/engpapers/3665>

Publication Details

Zhou, Y., Li, W., Zhang, X. & Kostidis, K. 2009, "Development of a force sensor working with MR elastomers", 2009 IEEE/ASME International Conference on Advanced Intelligent Mechatronics, AIM, IEEE, Singapore, pp. 233-238.

Research Online is the open access institutional repository for the University of Wollongong. For further information contact the UOW Library:
research-pubs@uow.edu.au

Development of a Force Sensor Working with MR Elastomers

Weihua Li, Kosta Kostidis, Xianzhou Zhang, and Yang Zhou

Abstract— This paper presents the development of a new force sensor with MR elastomer as a sensing element. One key element in this study was to find a suitable material with high sensing capabilities which can be used for developing a sensor. Thus different MR elastomers, with ingredients of carbonyl iron particle, graphite, silicone oil and silicone rubber, were manufactured and measured with a modified rheometer. The effects of additives on the sensing capabilities were systematically investigated and an optimal MR elastomer sample was selected for design and manufacturing of a force sensor prototype. The development sensor prototype consists of three units: mechanical unit, electrical circuit and LED display unit. The mechanical unit includes the MRE sample and the interface to the electronic circuit. A signal conditioning circuit was developed for calibrating output voltages, which are displayed on a LCD panel. The components of the electronic part were soldered on a board and communicate with the mechanical part for signal detection and testing. Overall the developed new MR elastomer based force sensor is able to detect external forces at the selected force ranges.

I. INTRODUCTION

Magnetorheological (MR) materials are a group of smart materials that consist of micro size magnetically polarisable particles suspended in a nonmagnetic matrix, i.e. viscous fluid (e.g. silicone oil) or elastomer matrix (e.g. silicone rubber)[1,2]. MR materials have their rheological and mechanical properties altered in the presence of a magnetic field. They exhibit a fast response to external stimuli, of the order of milliseconds. Up to now three main kinds of MR materials, including MR fluids, MR elastomers, and MR foams, have been reported. Amongst, MRs have proven to be commercially viable and suitable for many applications. The quick response, good reversibility and controllable performance make them widely used in various devices, such as dampers, clutches, and brakes [3-5]. However MR fluids exhibit a major shortcoming of particle sedimentation because of density mismatch between particles and the carrier fluid. This disadvantage is overcome by MR elastomers (MREs). Structurally, MREs are the solid analog of MR fluids, where the liquid oil is replaced by a natural or synthetic rubber matrix. Magnetizable particles, like iron particles, are embedded in the non conductive

rubber matrix. Silicon rubber, with a typical Si-O chain structure, is commonly used as matrix material, which keeps a high reversion rate of elasticity and low hysteretic loss during a broad range of temperature. This material also has advantages of good thermal stability, controlled thermal resistivity, low chemical reactivity, low toxicity and high flexibility [6]. However, this material tends to decrease the MR effect because of its relatively low magnetic permeability. Lokander and Stenberg [7] found that the matrix material plays an important role in contributing to the absolute MR effect. They concluded that the soft matrix material based MREs can generate higher MR effects than those of hard matrix MREs. Besides, other rubbers, such as nature rubbers, synthetic rubber, silicone rubber or some polyurethane were also used to fabricate MREs. [8-11].

The effects of physical and chemical properties of particle, including particle size, particle shape, volume fraction and particle magnetization, on the overall performance of MREs were studied by a number of researchers. Bellan and Bossis studied that the volume fraction of the particles influences the stress in relation to the strain [9]. Their study indicated that a higher volume fraction of magnetic particles were agglomerated in the rubber matrix so the matrix become stiffer and a higher stress must be applied to achieve the same strain as with lower volume fraction of particles. The maximum change in modulus increases monotonically with increasing volume percentage of iron. Jolly et al. reported that a higher volume fraction resulted in stronger interparticle forces because the gaps between particles show a decreasing trend with the volume fraction [12]. Lokander and Stenberg found that larger sizes of iron particles are easier to be aligned in the direction of the magnetic field, which will thus result in a higher MR effect [7].

Two different methods are commonly used for manufacturing MREs. One is room temperature vulcanizing and the other is heated vulcanization. The principle of both methods is similar. The components of the MREs are mixed and bubbles within the mixture are removed via a vacuum pump. Then the mixture is filled in a mold for curing. During curing, if a magnetic field is applied to the sample, the magnetic particles arrange in chains until the rubber base is cured and the particles are fixed in the matrix. This type of MRE sample is called an anisotropic MRE. Otherwise, if the MRE is cured without a magnetic field, it is called an isotropic MRE. In literature, both anisotropic [9,13] and isotropic [8,10] MREs were fabricated and their mechanical

All authors are with the School of Mechanical, Materials and Mechatronic Engineering, University of Wollongong, Wollongong, NSW 2522, Australia. Contact details of the corresponding author, Dr. Weihua Li, are: phone: 61 2 4221 3490; fax: 61 2 4221 3101; E-mail: weihuali@uow.edu.au.

properties have been investigated analytically and experimentally. Furthermore, these materials have found applications in developing vibration isolators [14-17]. It is noted that the majority MRE research is focused on the study of its magnetic field-dependent properties, like modulus and stiffness. But there are very limited researches studying the magnetostrictive properties of MREs. For an isotropic sample made of iron particles embedded in a silicon elastomer, Bossis et al. [18] observed a huge resistance change from about $5e+6$ to $0.7e+1$ when the magnetic field increased from 0 to 6000Oe. Also, in low resistance area a sharp reduce curve happened from around 3000Oe as well as a hysteresis loop can be observed. The phenomena that external magnetic field effectively decrease the resistance of MRE would lead a great future for this material in electronics and power systems. Guan et al. [19] studied the field-induced elongation of MRE samples and found the maximum magnetostriction could be as large as piezoelectric ceramics, which implies a promising application perspective. However, to our best knowledge, there isn't any work on the development of new sensors by using the magnetostrictive properties of MREs. This is the major motivation of this work.

This paper consists of two major parts. The first part is to fabricate, characterize and optimally select high performance MRE samples. The second part is to design, manufacture and test a sensor working with the MRE sample.

II. FABRICATION AND CHARACTERIZATION OF MRE SENSING PROPERTIES

A. Fabrication of MREs

The ingredients for fabrication of MRE samples are carbonyl iron powders (from BASF with the size of 3~5 μm), silicon rubber and graphite powers as additives. Ginder et al. [20] found that when the particle weight concentration is above 60%, the MRE sample will reach saturation. The following table shows 9 MRE samples, the particle weight ratios of which vary from 40% to 65%. As graphite powder and carbonyl iron particles are conductive solids compared with silicone rubber, they can be treated together as a conductive part of MRE. In addition, all these samples were classified as three groups: A, B, and C. For each group, the silicon rubber component is the same. Thus, the conducting part for these three groups are 60%, 70%, and 80%, respectively while the nonconductive parts are 40%, 30%, and 20%, respectively.

For each sample, carbonyl iron particles were first mixed with silicone rubber and then the graphite power is added into the mixture. A stirrer was used to make all the ingredients in a plastic container fully mixed with each other. Then, the mixture was filled in a mould and placed in a constant magnetic field of 1 Tesla for curing 24 hours at the

room temperature.

Table 1. Components of 9 MRE samples.

	A			B			C		
Carbonyl iron (3~5 μm)	35% 1.05g	40% 1.2g	50% 1.5g	40% 1.2g	45% 1.35g	55% 1.65g	50% 1.5g	55% 1.65g	65% 1.95g
Graphite power (12 μm)	25% 0.75g	20% 0.6g	10% 0.3g	30% 0.9g	25% 0.75g	15% 0.45g	30% 0.9g	25% 0.75g	15% 0.45g
Silicon rubber	40% 1.2g	40% 1.2g	40% 1.2g	30% 0.9g	30% 0.9g	30% 0.9g	20% 0.6g	20% 0.6g	20% 0.6g

B. Testing

The magnetostrictive properties of MRE sample were measured by using a modified MR rheometer, as shown in Fig. 1. The rheometer (model MCR301, Anton Paar Germany GmbH) is used to provide and measure strain, stress, normal force and magnetic field applied to MRE samples. For each testing, the MRE sample was sandwiched between the plates with a diameter of 20 mm. The upper plate was brought down towards the bottom plate to compress the sample. In all tests, the initial gap used was set as 1.45 mm as the sample thicknesses vary from 1.20mm 1.40mm. During compression, strain, stress, and resistance detection, no torsional motion was applied to the sample. The magnetic field is generated by a built-in MR cell [21]. An additional multi-meter is connected to the rheometer through a highly conductive copper clamp for testing resistances of the samples under various conditions, as shown in Fig. 1.

The application of the rheometer for testing mechanical and rheological properties of MR materials under various working modes were detailed in ref. [21]. In this experiment, the stepping loading and/or unloading method is applied to all samples. The normal force applied to the sample increases increase steadily from 0 N to 50 N with a step increment of 5 N. The time duration for each increment is 10 seconds. With this continuing loading method, the resistance of MR samples under different magnetic fields and loadings were measured.

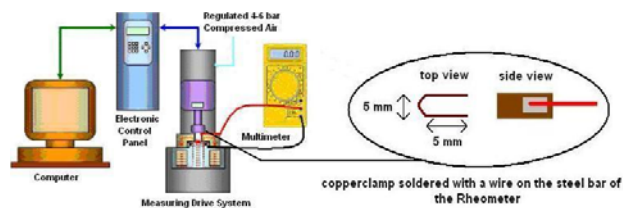


Fig. 1. Schematic diagram of the modified MR rheometer.

C. Results and Discussion

A number of experiments were conducted to test all 9 samples listed in Table 1. Amongst, one sample in group C, which has 55% carbonyl iron, 20% silicon rubber and 25% graphite powder, has the best performance. Fig. 2 shows the resistance of the sample versus the applied normal force

under various magnetic fields. It can be seen from this figure that the resistance responses consist of 3 distinct regions: I, II and III. Region I relates to low loading normal forces. In this region, the resistance is very high with the order of $M\Omega$ which can not be detected by the multimeter. Region II corresponds to the loading from 5N to 15N, where the MRE resistance shows a sharply decreasing trend. For example, without a magnetic field, the resistance changes from about 4.62 k Ω at the force of 5N to about 0.65 k Ω at the force of 15 N. The resistance change is more than 85%. Region III relates to the force above 15 N, where the resistance has almost no change with furthering increasing loading force. Comparing these three regions, only region II has good sensitivity, which will be selected to develop the proposed MRE force sensor.

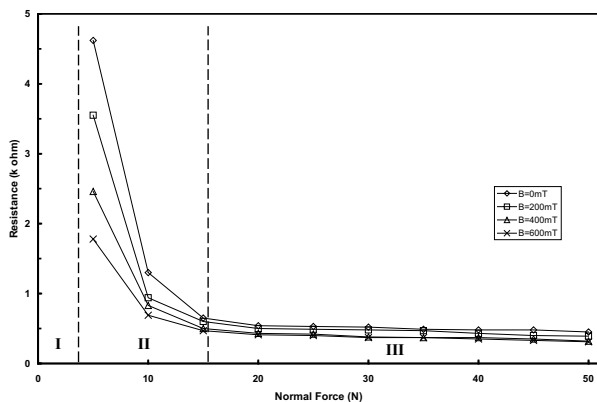


Fig. 2. Three regions of resistance versus normal force.

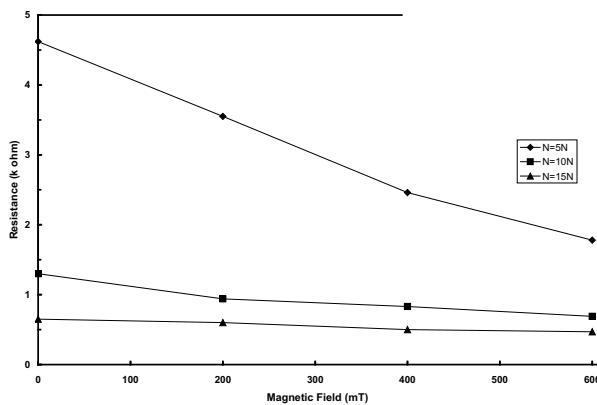


Fig. 3. Resistance versus magnetic field at different normal forces.

The effect of magnetic field on the resistance response is summarized and shown in Fig. 3. All the data were collected from experimental results in Fig. 2. Here, three typical normal forces, 5N, 10N, and 15N, were selected. Overall, the resistance of MRE samples shows a decreasing trend with magnetic field. This property could be explained by the field-induced particle motion. When the magnetic field increases, the particle magnetization increase and the attractive force between particles increase. These particles

tend to form a chain structure, which will result in the increment of conductivity or the decrease of the resistance. It is interesting to know that the decreasing rate is strongly dependent on the normal force applied to the material. At a normal force of 5N, the resistance decreases from 4.62 k Ω without a magnetic field to 1.78 k Ω at the magnetic field of 600 mT. The decreasing rate is more than 60%. This result also demonstrates that the MRE sample could be used to develop a sensor for measuring magnetic fields. This result indicates that the detection is very sensitive to the normal force. When the normal force is 15N, the field-induced resistance only has less than 28% change from 0.65 k Ω at 0 mT to 0.47 k Ω at 600 mT.

III. DESIGN, MANUFACTURING AND TESTING OF A MRE SENSOR

A. Mechanical Design

The whole MRE force sensor system consists of three parts: mechanical part, electrical circuit and the LED display part. The schematic of the mechanical part is shown in Fig. 4 (a). The mechanical design consists of 8 components. The base holder is used to connect all the parts together and separate the electrodes. Both the lower plate and the upper plate work as electrodes. The lower plate is fixed on the base holder with strong adhesive. The MRE sample is placed between the lower plate and the button. When the upper plate is screwed, the O-ring made of rubber material can provide the button a preload. Therefore, the preload can be applied on the MRE sample for a primary deformation. In addition, the preload can be adjusted by screwing or unscrewing the upper plate. The metal spring is pressed to get a primary deformation. This spring provides a recovery force to the sensor. The picture of the mechanical prototype is shown in Fig. 4 (b).

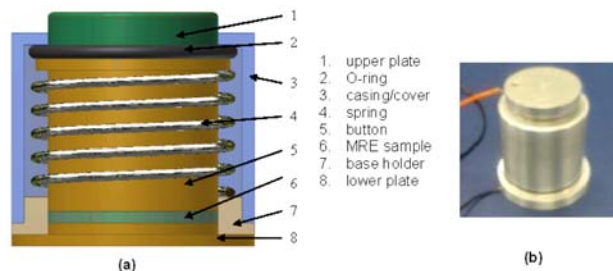


Fig. 4. (a) Schematic design of the MRE force sensor; (b) picture of the sensor prototype.

B. Modeling and Characterization

The working mechanism as well as the force analysis is shown in Fig. 5. Initially, the button doesn't connect the MRE sample as the spring recovery force, F_s is larger than the sum of the button weight and the upper plate, F_b . The casing responsive force F_c is used to balance the part of the spring force. i.e. $F_s = F_b + F_c$. F_w is a preload used for

pushing the button downwards to contact the MRE sample. A critical value of the preload is $F_w(cr)=F_b$. When the critical preload is applied to the button, the casing response force just disappears. If the applied preload is larger than the critical value, the button would generate a normal force to the MRE sample. Besides the preload, the external force F_1 will result in the further deformation of the MRE sample, which can be detected by the MRE resistance change.

For our developed prototype, as shown in Fig. 4 (b), the mass of the button and the upper plate is 102.8 g. Thus, the critical preload $F_w(cr)= 102.8 \text{ g} * 9.8 \text{ N/kg} = 1.0084 \text{ N}$. When the preload is applied to the system, the button will reach the position 1 as shown in Fig. 5. In our design, the distance from the position 1 to the lower plate is 2mm. The MRE sample thickness in the developed sensor is 1.32mm. Thus, additional preload should be applied to make sure that the button connects with the MRE sample. After calculation, 0.0938 N is needed. In short, for this prototype, the preload of 214.5 g or 2.1022 N is applied to make sure the button just reach the position 2 (Fig. 5).

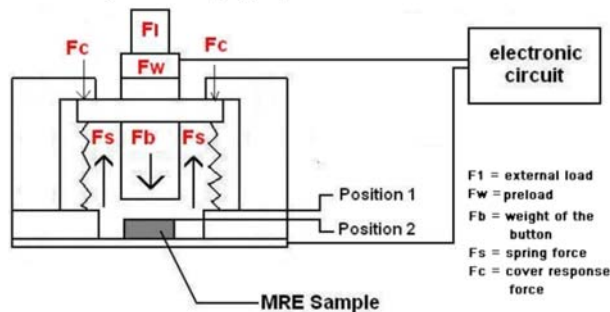


Fig. 5. Modeling analysis.

C. Electrical Circuits

The whole electrical circuits consist of three parts: (a) the calibration circuit, (b) the wave indicator circuit, and (c) the LCD display unit, as shown in Fig. 6.

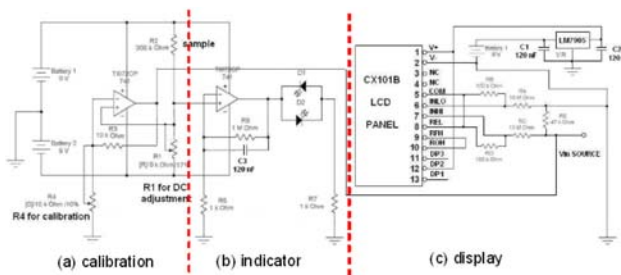


Fig. 6. Electrical circuits.

Calibration unit: The calibration circuit part is important to calibrate the output signal. For simulation purpose the resistance $R_1=200k\Omega$ is supposed to be the MRE sample. Then the $20k\Omega$ resistance can be replaced by the mechanical device which includes the MRE sample. The two 9V batteries are used to provide energy to the electrical circuit. The operation amplifier TL072CP is in an 8 pin

package format, which has two amplifiers and a maximum supply voltage of $\pm 18V$. Also, it has a high input resistance of 1012Ω which can easily protect the input ports from high current. The slew rate with $13V/\mu s$ is very high, which is significant for detecting fast wave signals. In this calibration unit, the operation amplifier is working as a gain amplifier. The amplifier consist of an inverting input and a non inverting input, where only the difference in voltage between the two ports appears. The amplifier is designed to be used in a negative-feedback configuration, where the desired gain is controlled by a resistive voltage divider feeding a fraction of the output voltage to the inverting input of the operational amplifier. In this circuit the feedback loop consist of the resistance $R_3 = 10k\Omega$ and $R_4 = 10k\Omega$. R_4 is a potentiometer that can be adjusted for calibrating the output signal. In case of altering the resistance R_4 , the gain will be changed and a calibration is possible. If no calibration is necessary then R_4 can be set to zero.

Indicator unit: In this unit, two Light Emitting Diode (LEDs) D1 red and D2 green can display when a wave signal has a positive or a negative value. If no force is applied to the MRE sample, both LEDs are switched off. Otherwise, the wave signal can be provided by applying a sinusoidal force on the MRE device where the MRE sample is housing.

The frequency of the wave signal can be estimated by counting the flashing light of the LED. The zero point can be adjusted by using a resistor $R_1=5k\Omega$ as a potentiometer. The resistance R_2 will be later replaced by the MRE sample, the resistance change of which can change the output voltage. The operation amplifier is acting here as a gain amplifier. The gain is provided by the feedback circuit where resistors R_6 and R_5 are included. Resistor R_6 is 1000 times higher than R_5 , which means that the amplifier has a high gain and the output signal is very sensitive compared to the input signal. Small alteration of the input signal will result in a high change of the output signal. R_7 with $1k\Omega$ is used to protect the two LEDs from high current. Capacitor C_3 is a decoupling capacitor which is used to reduce the effect of noise caused by other circuit elements from the rest of the circuit.

LED display: For displaying the values, the c+c miniature 3-1/2 digit LCD digital panel meter cx101 is used. The cx101B series are convincing with features of high reliability, good quality and low price. A recommended support circuit for using the LCD display is shown in Fig. 6 (c). In this unit, four pins (5,6,7, 8) and associated electrical circuits are used to measure the current of signals. In particular, two voltage dividers with the resistors R_B/R_A and R_C/R_D as well as the input pins 6 and 7 are connecting to realize the measurement function. On pin 1 and 2 the power supply can be attached. The three decimal points are selected by simple pinstripping. Pin 13 short-circuiting pin 1 lights the decimal point left to hundreds digits, pin 12 lights the

decimal point to tens digits and pin 11 to units digits. Here port 12 is used for setting the decimal point on the display. In addition, the LM7905 series of voltage regulators and the decoupling capacitors C1 and C2 ensure to provide right voltages to input pins.

D. Prototyping Testing

As discussed in section 3.2, the preload is necessary for effectively testing force-resistance relationship. The analysis and calculation in section 3.2 indicated that the preload for just contacting the MRE sample is 214.5 g or 2.1022 N. However, with this low preload, the resistance of this device is very high, which cannot get well calibration and accurate reading. The reason why a calibration is hard is partially because of the operation amplifier in the calibration electrical circuit. Considering all possible reasons, it was suggested that that an optimal calibration is in a range from 300g to 1000g. We have conducted a number of testing and comparison and found the preload of 500g is an optimal value for this prototype. With this preload, the output voltage against external loads, ranging from 0g to 700g (or from 0N to 6.87N) were measured and shown in Fig. 7 (solid line). The results shows a favorably linear relationship, which demonstrates that the first MRE sensor performance is very good.

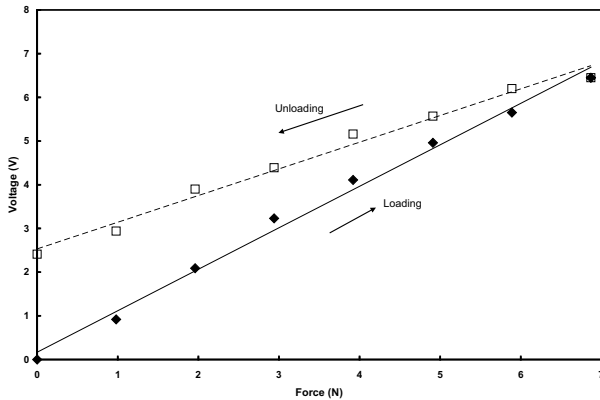


Fig. 7. Relationship between the output voltage and the external loading.

It is noted that the result is just for loading case, where the external loading increases from 0 to a maximum value. We also tested the system response under unloading case when the external loading was reduced from the maximum value to the zero, which is shown in the figure (dashed line). Obviously, the unloading case is quite different from the loading case though the response also follows a good linearly decreasing trend. This result indicates that the MRE material doesn't have a good recovery property, which was also reported by Guan et al. [19]. With the current material status, it is quite challenging to develop effective and reliable MRE sensors. Thus, the material design would play a key role in this research. Other approaches could also

compensate for the material performances.

IV. DISCUSSION AND FUTURE WORK

We fabricated, for the first time, a force sensor by using the sensing capabilities of MR elastomers. However, there exist a number of important tasks ahead for its practical applications or commercialization. A few important issues have been figured out and a few important tasks are now being implemented. Current and future work is summarized below.

(a) Fabrication of new MRE materials with higher sensing capabilities and better repeatability. Besides carbonyl iron particles based MREs, we would also try to select and fabricate other magnetizable particles, such as pure iron or iron alloy, based MREs and study their sensing properties. Stability and repeatability of MRE samples are important issues for practical applications. Besides materials development, other properties, like creep and recovery, stress relaxation, will be experimentally and theoretically investigated. These understandings will be very useful for studying stability and repeatability of MRE materials as well as MRE devices.

(b) A microcontroller will be used as a sensor. The signal acquisition and processing will also be developed in a compact board.

(c) The reported results were measured under steady-state condition. The dynamic properties of the MRE sensor will be experimentally studied with an impedance analyzer. A mathematical model will also be developed to evaluate the sensor performances.

(d) The current prototype demonstrated the concept that MRE can work as a force sensor. However, the MR effect on the sensing capability hasn't been well discussed. Our future work will address this problem.

V. CONCLUSION

This project aims to study sensing capabilities of MREs and study its applications. A series of carbonyl particle/graphite powder/silicone rubber based MRE samples were fabricated and their resistance properties against external forces at various magnetic fields were studied. It was found that the MRE sample with the composition (55% carbonyl iron + 20% silicon rubber + 25% graphite powder) had the best sensing capability. In particular, its resistance has more than 85% changes when the normal force increased from 5 N to 15 N. With this sample working as a sensing element, a force sensor prototype was designed and manufactured. The device consists of three units: the calibration unit, the indicator unit and the LED display. With a careful selection of the preload of 500g for calibration, the system shows a nice linear relationship between the output voltage with the input

loading force. This study did demonstrate the new MRE applications though there still exists many challenging works.

ACKNOWLEDGMENT

This work was supported by the University of Wollongong through a URC small grant. The authors appreciate excellent comments from anonymous reviewers on the improvement of this paper.

REFERENCES

- [1] J.D. Carlson, M.R. Jolly, "MR fluid, foam and elastomer devices, *Mechatronics*, (2000) 10, 555–569.
- [2] W.H. Li, H. Du, G. Chen, S.H. Yeo, N.Q. Guo, Nonlinear rheological behavior of magnetorheological fluid: step-strain experiments, *Smart Materials & Structures* (2002), 11 (2), 209-217.
- [3] X.J. Wang, F. Gordaninejad, Flow analysis and Modeling of field-controllable, electro- and magneto-rheological fluid dampers, *Journal of Applied Mechanics- Transactions of the ASME* (2007), 74 (1), 13-22.
- [4] B. Liu, W.H. Li, P.B. Kosasih, X.Z. Zhang, Development of an MR-brake-based haptic device, *Smart Materials and Structures* (2006), 15 (6), 1960-1966.
- [5] W.H. Li, H. Du, N.Q. Guo, Design and analysis of a magnetorheological brake, *International Journal of Advanced Manufacturing Technology* (2003), 21 (7), 508-515.
- [6] J. A Brydson, *Plastics materials*, 9th Ed, Butterworth-Heinemann, 1999.
- [7] M. Lokander, B. Stenberg, Improving the magnetorheological effect in isotropic magnetorheological rubber materials, *Polymer Testing*, (2003) 22,677–680.
- [8] Y.L. Wang, Y.A. Hu, L. Chen, et al., Effects of rubber/magnetic particle interactions on the performance of magnetorheological elastomers, *Polymer Testing* (2006), 25 (2), 262-267.
- [9] C. Bellan, G. Bossis, Field dependence of viscoelastic properties of MR elastomers, *International journal of modern physics B* (2002) 16, 17&18, 2447–2453.
- [10] X.L. Gong, X.Z. Zhang, P.Q. Zhang, Fabrication and characterization of isotropic magnetorheological elastomers, *Polymer Testing* (2005), 24(5), 669-676.
- [11] L. Flandin, A. Hiltner and E. Baer, Interrelationships between electrical and mechanical properties of a carbon black-filled ethylene-octene elastomer, *Polymer* (2001), 42, 827–838.
- [12] M.R. Jolly, J.D. Carlson, B.C. Munoz, A model of the behaviour of magnetorheological materials, *Smart Materials & Structures* (1996), 5 (5), 607-614.
- [13] G.Y. Zhou, Shear properties of a magnetorheological elastomer, *Smart Materials and Structures*, (2003) 12(1), 139-146.
- [14] D. York, X. Wang, F. Gordaninejad, A new MR fluid-elastomer vibration isolator, *Journal of Intelligent Material Systems and Structures* (2007), 18, 1221-1225.
- [15] H.X. Deng, X.L. Gong and L.H. Wang, Development of an adaptive tuned vibration absorber with magnetorheological elastomer, *Smart Materials and Structures* 15 (2006), N111–N116.
- [16] A.A. Lerner, K.A. Cunefare, Performance of MRE-based vibration absorbers, *Journal of Intelligent Material Systems and Structures* (2008), 19 (5), 551-563.
- [17] N. Zhang, N. Hoang, H.P. Du, A novel dynamic absorber using enhanced magnetorheological elastomers for powertrain vibration control, *Advanced Materials Research* (2008), 47-50, 117-120.
- [18] G. Bossis, C. Abbo, S. Cutillas, S. Lacis, C. Metayer, Electroactive and electrostructured elastomers, *International Journal of Modern Physics B* (2001), 15 (6-7), 564-573.
- [19] X.C. Guan, X.F. Dong, J.P. Ou, Magnetostrictive effect of magnetorheological elastomer, *Journal of Magnetism and Magnetic Materials* (2008), 320 (3-4), 158-163.
- [20] J.M. Ginder, S.M. Clark, W.F. Schlotter, M.E. Nichols, Magnetostrictive phenomena in magnetorheological elastomers (2002), *International Journal of Modern Physics B*, 16 (17-18), 2412-2418.
- [21] W.H. Li, H. Du, N.Q. Guo, Dynamic behavior of MR suspensions at moderate flux densities, *Materials Science and Engineering A* (2004), 371(1-2), 9-15.